

**Rydberg states of 7Li_2 by pulsed optical–optical double resonance spectroscopy:
Molecular constants of 7Li_2 +**

R. A. Bernheim, L. P. Gold, and T. Tipton

Citation: *The Journal of Chemical Physics* **78**, 3635 (1983); doi: 10.1063/1.445192

View online: <http://dx.doi.org/10.1063/1.445192>

View Table of Contents: <http://scitation.aip.org/content/aip/journal/jcp/78/6?ver=pdfcov>

Published by the [AIP Publishing](#)

Articles you may be interested in

[Perturbation facilitated optical–optical double resonance spectroscopy of the \$23\Sigma^+ g\$, \$33\Sigma^+ g\$, and \$43\Sigma^+ g\$ Rydberg states of \$7\text{Li}_2\$](#)

J. Chem. Phys. **102**, 3024 (1995); 10.1063/1.468612

[A pulsed optical–optical double resonance study of the \$11\Pi g\$ state of \$7\text{Li}_2\$](#)

J. Chem. Phys. **92**, 5822 (1990); 10.1063/1.458402

[Optical–optical double resonance spectroscopy of molecular ions](#)

J. Chem. Phys. **76**, 4720 (1982); 10.1063/1.442789

[A study of the \$E\ 1\Sigma^+ g\$ state of \$7\text{Li}_2\$ by pulsed optical–optical double resonance spectroscopy](#)

J. Chem. Phys. **76**, 57 (1982); 10.1063/1.442705

[A spectroscopic study of the \$G\ 1\Pi g\$ state of \$7\text{Li}_2\$ by pulsed optical–optical double resonance](#)

J. Chem. Phys. **74**, 2749 (1981); 10.1063/1.441444



Rydberg states of ${}^7\text{Li}_2$ by pulsed optical-optical double resonance spectroscopy: Molecular constants of ${}^7\text{Li}_2^+$

R. A. Bernheim,^{a)} L. P. Gold, and T. Tipton

Department of Chemistry, Davey Laboratory, The Pennsylvania State University, University Park, Pennsylvania 16802

(Received 10 August 1982; accepted 6 September 1982)

Three Rydberg series of electronic states of ${}^7\text{Li}_2$ have been characterized by pulsed optical-optical double resonance spectroscopy. The observed Rydberg states, which include the previously reported $E^1\Sigma_g^+$ and $G^1\Pi_g$ states, have been identified as $3-10s\sigma^1\Sigma_g^+$, $3-10d\sigma^1\Sigma_g^+$, and $3-15d\pi^1\Pi_g$. The molecular constants for several of the upper members of each of the above series have been used to deduce the ionization potential of ${}^7\text{Li}_2$ and molecular constants for the $X^2\Sigma_g^+$ state of ${}^7\text{Li}_2^+$. The former was determined to be $T_0(\infty) = 41\,496 \pm 4\text{ cm}^{-1}$. The latter were found to be in good agreement with recent *ab initio* calculations.

I. INTRODUCTION

The lithium dimer is of considerable interest to theoreticians since it is the least complex stable homonuclear diatomic molecule after H_2 . However, prior to the beginning of the investigation of Li_2 in this laboratory in 1979, only five electronic states of this molecule were characterized experimentally. These factors provided the impetus for undertaking a new spectroscopic investigation of Li_2 of which this paper is a part.

The method of pulsed optical-optical double resonance spectroscopy (OODR) has previously been used¹⁻⁵ to study several excited *gerade* electronic states of ${}^7\text{Li}_2$. More recently it has been used to characterize members of three Rydberg series of ${}^7\text{Li}_2$, and some preliminary findings of this work have been reported earlier.⁶ This paper presents results for 28 *gerade* states lying in the range of $33\,000\text{--}42\,000\text{ cm}^{-1}$ above the ground electronic state. The molecular constants obtained for these states were extrapolated to yield corresponding constants for the ground state of Li_2^+ and an accurate ionization potential for the neutral molecule. The former are the first experimentally determined spectroscopic properties of the ground state of Li_2^+ although a number of theoretical studies of this molecular ion have been made.^{7,8}

The three sets of *gerade* Rydberg states that have been identified in Li_2 consist of the lowest 13 members ($n=3\text{--}15$) of an $nd\pi^1\Pi_g$ series and the lowest eight members ($n=3\text{--}10$) of an $nd\sigma^1\Sigma_g^+$ and an $ns\sigma^1\Sigma_g^+$ series. Only Rydberg states of $^1\Sigma_g^+$ and $^1\Pi_g$ symmetry were accessible since the second step of all of the OODR excitations originated at the $A^1\Sigma_u^+$ state. The T_e values of these states as well as those of all other previously observed states of Li_2 are shown schematically in Fig. 1. The latter include three *gerade* states investigated earlier in this laboratory: $E^1\Sigma_g^+$, $G^1\Pi_g$, and $F^1\Sigma_g^+$.¹⁻⁵ The $E^1\Sigma_g^+$ and $G^1\Pi_g$ states were determined to be the lowest members of the $ns\sigma^1\Sigma_g^+$ and $nd\pi^1\Pi_g$ Rydberg series, respectively. The $F^1\Sigma_g^+$ state correlates with the doubly excited $\text{Li}(2p) + \text{Li}(2p)$ configuration.

^{a)}Visiting fellow, 1981-82, Joint Institute for Laboratory Astrophysics, University of Colorado and National Bureau of Standards, Boulder, Colorado 80309.

II. EXPERIMENTAL

The experimental apparatus has previously been described in detail.¹⁻³ Two tunable dye lasers were pumped by the divided output beam of a nitrogen laser. The output beams of the dye lasers overlapped one another in a heat pipe cell containing Li_2 vapor. OODR excitations were produced by pumping a single $A^1\Sigma_u^+ \rightarrow X^1\Sigma_g^+$ transition with one dye laser and scanning through the range $530\text{--}370\text{ nm}$ with the second dye laser. The short wavelength limit of the latter "probe" laser range was determined by spectral intensity factors rather than by the extent of the tuning range of the laser. The probe laser pulse was optically delayed to allow a limited amount of collision-induced rotational relaxation to take place in the intermediate state before the second step of the OODR excitations. The extra transitions which

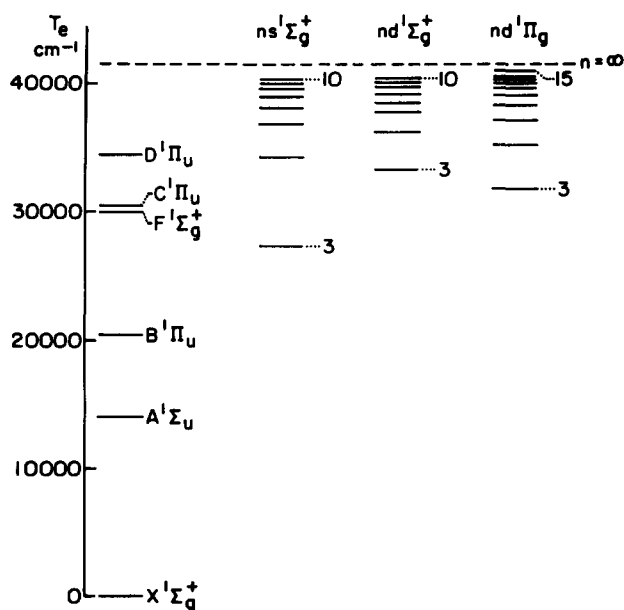


FIG. 1. The electronic energies T_e of all experimentally observed states of ${}^7\text{Li}_2$. The three Rydberg series that are reported in this work are shown in columns 2-4 of this figure. All other observed states appear in column 1. The broken horizontal line denotes the calculated location of the ionization limit of ${}^7\text{Li}_2$.

TABLE I. Dunham coefficients (cm^{-1} units) for the Rydberg $nd\pi^1\Pi_g$ states. Standard deviations are given in parentheses. For $n=7-11$, the Π^- and Π^+ components were fitted separately. The Y_{02} values listed for the $10d\pi^1\Pi_g^-$ and $11d\pi^1\Pi_g^-$ components were estimated using Eq. (7), and then incorporated into the Dunham fits.

n	T_g	Y_{10}	Y_{20}		
4	35 360.761 (0.05)	228.9824 (0.06)	-2.129 79 (0.02)		
5	37 257.700 (0.05)	237.3867 (0.04)	-1.608 74 (0.007)		
6	38 460.909 (0.05)	249.2891 (0.05)	-1.565 09 (0.008)		
7 -	39 249.495 (0.3)	253.8988 (0.6)	-1.181 32 (0.2)		
7 +	39 248.478 (0.07)	255.0904 (0.09)	-1.506 79 (0.03)		
8 -	39 779.262 (0.2)	257.3414 (0.4)	-1.325 37 (0.1)		
8 +	39 779.001 (0.1)	257.7284 (0.1)	-1.466 59 (0.04)		
9 -	40 150.674 (0.01)	253.8808 (0.01)	-0.447 08 (0.004)		
9 +	40 142.275 (0.3)	261.1221 (0.2)	-1.961 16 (0.07)		
10 -	40 415.804 (0.5)	263.7765 (0.8)	-1.865 28 (0.3)		
10 +	40 414.932 (0.3)	261.3922 (0.3)	-1.441 48 (0.1)		
11 -	40 609.962 (0.2)	259.1735 (0.3)	-1.256 76 (0.09)		
11 +	40 606.600 (0.2)	261.7270 (0.2)	-1.567 65 (0.05)		
n	$Y_{30} \times 10^2$	Y_{01}	$Y_{11} \times 10^3$	$q \times 10^3$	
4	-2.6759 (0.2)	0.474 485 3 (0.000 08)	-7.361 77 (0.01)	0.8315 (0.03)	
5		0.479 406 9 (0.0001)	-5.938 28 (0.02)	1.9305 (0.04)	
6		0.485 969 9 (0.000 09)	-5.278 02 (0.02)		
7 -		0.491 286 9 (0.0006)	-5.342 46 (0.3)		
7 +		0.472 754 9 (0.0002)	-4.908 69 (0.02)		
8 -		0.494 902 6 (0.0004)	-4.700 64 (0.2)		
8 +		0.466 360 7 (0.0005)	-4.396 67 (0.04)		
9 -		0.495 008 8 (0.000 02)	-3.965 18 (0.01)		
9 +		0.483 489 2 (0.0005)	-3.796 13 (0.09)		
10 -		0.496 038 9 (0.001)	-7.088 92 (0.9)		
10 +		0.455 625 9 (0.001)	-4.894 57 (0.2)		
11 -		0.496 345 4 (0.0005)	-3.912 18 (0.3)		
11 +		0.481 183 7 (0.0005)	-4.147 80 (0.2)		
n	$Y_{02} \times 10^6$	$Y_{03} \times 10^9$	$Y_{04} \times 10^{12}$		
4	-7.863 59 (0.04)				
5	-7.338 19 (0.04)				
6	-6.521 03 (0.05)				
7 -	-6.779 49 (0.3)				
7 +	4.335 94 (0.3)	-3.277 50 (0.1)	0.400 65 (0.02)		
8 -	-6.875 97 (0.3)				
8 +	13.989 19 (0.9)	-7.409 25 (0.6)	1.036 67 (0.1)		
9 -	-6.817 28 (0.007)				
9 +	-1.635 52 (0.5)	-0.854 94 (0.2)			
10 -	-7.1				
10 +	36.501 69 (2)	-15.656 33 (1)			
11 -	-7.1				
11 +	3.036 38 (0.4)				

resulted permitted an expanded spectral data base while preserving the unambiguous spectral assignment characteristics of the pulsed OODR experiment. The pump and probe lasers produced output powers of 75 and 60–300 $\mu\text{J}/\text{pulse}$, respectively, under the experimental conditions used.

The heat pipe oven was loaded with several grams of lithium (99.99% ${}^7\text{Li}$) and 30 Torr of He at room temperature. An operating temperature of 650°C was used for the study of Rydberg states up to $n=6$; 730°C was used for higher states to compensate for the decrease in transition probability as n increases. At 650°C , the partial pressures of the gaseous species in the heat pipe are estimated to have been 90 Torr He, 0.002 Torr Li_2 , and 0.2 Torr Li; the corresponding estimates at

730°C are 100 Torr He, 0.02 Torr Li_2 , and 0.7 Torr Li.

Excitation to Rydberg states was detected by monitoring the ultraviolet emission from the heat pipe cell. This emission was due, at least in part, to collisional transfer of energy from *gerade* to nearby *ungerade* states followed by single-photon transitions to the ground state.⁴ The linewidths of the resulting OODR spectra were typically 0.7 cm^{-1} .

Calibration of the spectra was achieved by sampling portions of the probe beam with neon and argon optogalvanic cells and a Fabry–Perot interferometer. Spectral and calibration data were recorded both on a chart recorder and in digital form.

The only significant revision of the earlier experi-

TABLE II. Dunham coefficients (cm^{-1} units) for the Rydberg $n\sigma^1\Sigma_g^+$ states. Standard deviations are given in parentheses.

n	T_e	Y_{10}	Y_{20}
4	34 293.643 (0.07)	270.7360 (0.09)	-2.923 66 (0.04)
5	36 832.622 (0.04)	249.4297 (0.07)	-2.934 25 (0.02)
6	38 129.130 (0.1)	251.7842 (0.2)	-4.085 97 (0.07)
7	39 007.312 (0.1)	260.5552 (0.2)	-1.918 11 (0.05)
8	39 624.361 (0.05)	262.5268 (0.06)	-1.628 86 (0.02)
9	40 044.034 (0.2)	262.0960 (0.2)	-1.491 64 (0.06)
10	40 339.509 (0.09)	262.6953 (0.1)	-1.618 11 (0.08)
n	$Y_{30}\times 10^2$	Y_{01}	$Y_{11}\times 10^3$
4	-8.1534 (0.4)	0.479 691 8 (0.0001)	-6.278 68 (0.06)
5		0.489 765 1 (0.000 08)	-10.005 85 (0.04)
6		0.485 693 3 (0.0005)	-9.883 52 (0.3)
7		0.495 830 4 (0.0002)	-4.440 20 (0.06)
8		0.491 598 0 (0.000 06)	-5.338 64 (0.02)
9		0.490 847 7 (0.0005)	-4.402 24 (0.2)
10		0.480 810 7 (0.0006)	-6.843 30 (0.5)
n	$Y_{21}\times 10^4$	$Y_{02}\times 10^6$	$Y_{03}\times 10^9$
4	-2.830 31 (0.1)	-6.1618 (0.04)	
5		-7.6376 (0.03)	
6		-8.6932 (0.4)	
7		-8.2105 (0.2)	0.260 38 (0.04)
8		-6.6164 (0.02)	
9		-10.8119 (0.7)	2.553 03 (0.3)
10		-1.1051 (0.7)	
n	$Y_{04}\times 10^{12}$		
4			
5			
6			
7			
8			
9	-0.415 160 (0.05)		
10			

mental procedures was the introduction of a new dye mixture to the pump laser. It was found that the combination of the dye LD700 and DCM produces at least three times as much power⁹ throughout the range 680–780 nm than can be obtained with any previously reported¹⁰ dye solution pumped by a nitrogen laser. The gain curve of this mixture can be peaked at any wavelength in the range 650–750 nm by adding varying amounts of LD700 to a solution containing 0.9 mg/ml DCM in 80% DMSO/20% ethanol.

III. ANALYSIS

The data consist of approximately 2800 transitions¹¹ from the $A^1\Sigma_u^+$ state to 28 electronic states lying in the range 33 000–42 000 cm^{-1} above the bottom of the ground state potential well. Only levels $v=0, 1, 2$, and 4 of the intermediate $A^1\Sigma_u^+$ state were pumped since these were sufficient to establish vibrational numberings in the Rydberg states and to yield adequate data bases for the determination of low-order molecular constants. For each Rydberg state reported in this work, data have been obtained for at least $v^*=0, 1$, and 2. The highest observed vibrational level for any of these Rydberg states was $v^*=7$. Most of the OODR transitions terminated on rotational levels within the range $J^*=0$ –40, although levels up to $J^*=59$ were observed in some instances.

The vibrational numbering was initially assigned to each state by assuming that the lowest observed level is $v^*=0$. In all cases, the lowest observed vibrational level seen while pumping $v'=1, 2$, or 4 in the $A^1\Sigma_u^+$ state was no lower than the lowest level seen from $v'=0$. Franck-Condon factors were derived from the Dunham coefficients for states $n=4$ –11 of the $nd\pi^1\Pi_g^+$ series, $n=3$ –6 of the $n\sigma^1\Sigma_g^+$ series, and $n=3$ –5 of the $nd\sigma^1\Sigma_g^+$ series. In all cases, the initial assignments were confirmed by comparisons of the Franck-Condon factors with the observed relative band intensities. Several high-lying observed members of the $nd\pi^1\Pi_g^+$, $n\sigma^1\Sigma_g^+$, and $nd\sigma^1\Sigma_g^+$ series could not be used in this analysis because of the substantial influence of $\Sigma^+\leftrightarrow\Pi^+$ lambda-doubling perturbations on the rotational constants of these states. However, since Franck-Condon factors for transitions originating from the $A^1\Sigma_u^+$ state are expected to become nearly independent of n and Λ at large n , the factors derived for the high-lying $^1\Pi_g^+$ components ought to apply to the nearby $^1\Pi_g^+$ components and $^1\Sigma_g^+$ states as well. The experimental observations qualitatively confirm this expectation.

The measured wavelengths were converted to energies referred to the bottom of the $X^1\Sigma_g^+$ state potential using the $A^1\Sigma_u^+$ state constants of Kusch and Hessel.¹² The

TABLE III. Dunham coefficients (cm^{-1} units) for the Rydberg $nd\sigma^1\Sigma_g^+$ states. Standard deviations are given in parentheses.

n	T_e	Y_{10}	Y_{20}
3	33 320.180 (0.04)	248.6108 (0.06)	-3.070 61 (0.03)
4	36 284.875 (0.07)	263.2002 (0.1)	-3.656 64 (0.03)
5	37 890.096 (0.1)	145.6560 (0.3)	23.021 41 (0.1)
6	38 571.788 (0.1)	247.5540 (0.09)	-1.051 37 (0.02)
7	39 277.230 (0.3)	261.5741 (0.5)	-2.044 38 (0.2)
8	39 798.738 (0.2)	261.0142 (0.2)	-1.634 25 (0.06)
9	40 163.871 (0.2)	262.2483 (0.2)	-1.741 67 (0.05)
10	40 426.921 (0.3)	261.9442 (0.3)	-1.418 24 (0.1)
n	$Y_{30}\times 10^2$	$Y_{40}\times 10^2$	Y_{01}
3	18.3739 (0.5)	-1.120 34 (0.03)	0.465 379 5 (0.000 07)
4			0.493 545 7 (0.0001)
5	-239.3077 (2)		0.476 010 4 (0.0002)
6			0.497 241 8 (0.0005)
7			0.512 108 4 (0.0006)
8			0.528 592 2 (0.0006)
9			0.534 257 7 (0.0008)
10			0.545 990 0 (0.001)
n	$Y_{11}\times 10^3$	$Y_{21}\times 10^4$	$Y_{31}\times 10^5$
3	-2.857 77 (0.04)	0.046 59 (0.1)	-2.846 01 (0.1)
4	-5.436 16 (0.1)	-6.037 26 (0.4)	
5	-10.423 65 (0.3)	16.760 32 (0.6)	
6	-4.413 31 (0.2)		
7	-4.392 25 (0.2)		
8	-5.792 98 (0.1)		
9	-6.177 89 (0.1)		
10	-5.542 91 (0.3)		
n	$Y_{02}\times 10^6$	$Y_{12}\times 10^6$	$Y_{03}\times 10^9$
3	-6.5530 (0.06)	-0.181 82 (0.007)	0.099 22 (0.02)
4	-7.2513 (0.04)		
5	-10.9856 (0.1)	2.077 68 (0.08)	
6	-9.0409 (0.6)	1.669 52 (0.2)	-0.749 08 (0.09)
7	-10.0650 (0.5)		0.440 18 (0.1)
8	-18.1594 (0.7)		2.123 25 (0.2)
9	-22.6178 (1)		3.715 39 (0.4)
10	-33.4130 (2)		

assigned data for each electronic state were fitted by a linear least squares procedure with the conventional Dunham expansion:

$$\nu(v, J) = \sum_{n,k} Y_{nk} (v + \frac{1}{2})^n [J(J+1) - \Lambda^2]^k, \quad (1)$$

where the symbols Y_{nk} , v , J , and Λ have their usual meanings. For the P and R branches of the ${}^1\Pi_g$ states, the term $q[J(J+1)-1]$ was appended to Eq. (1) in order to describe lambda-doubling interactions. The quantity q in this term is the lambda-doubling constant. The Dunham coefficients obtained from the above fits are presented in Tables I-IV. Digits beyond the determined standard deviations are given for each coefficient to compensate for the effects of statistical correlations. Dunham coefficients were not calculated for the observed $n=12-15$ states of the $nd\pi^1\Pi_g$ series because of limited data.¹³ The term values and limited vibrational constants for these four states are given later in Tables VI and VII. The standard deviations of the Dunham fits and extents of the corresponding data bases are indicated in Table V.

The statistical analyses of the $7-11d\pi^1\Pi_g$ states were hampered by a scarcity of Π^- data resulting from the inability of the probe laser to resolve lines in the Q branches of the observed $nd\pi^1\Pi_g \leftarrow A^1\Sigma_u^+$ transitions. It was found that the Π^- and Π^+ data of these states cannot be fitted with a single Dunham expansion without the

TABLE IV. Dunham coefficients (cm^{-1} units) for an observed ${}^1\Pi_g$ state of ${}^7\text{Li}_2$ having an unidentified atomic correlation.

Constant	Value (Std. Dev.)
T_e	38.849.420 (0.07)
Y_{10}	260.4173 (0.09)
Y_{20}	-1.644 61 (0.03)
Y_{01}	0.504 205 0 (0.000 09)
$Y_{02}\times 10^6$	-7.422 73 (0.03)
$Y_{11}\times 10^3$	-6.169 85 (0.03)

TABLE V. Statistical data for the Rydberg states of diatomic lithium.

n	Maximum ν	Maximum J	Std. dev. of fit (cm^{-1})	Number of lines fit
$ns\sigma^1\Sigma_g^+$ series				
4	5	45	0.20	271
5	3	49	0.12	145
6	2	31	0.14	35
7	2	59	0.27	136
8	2	49	0.08	73
9	2	57	0.21	78
10	2	25	0.06	17
$nd\sigma^1\Sigma_g^+$ series				
3	7	51	0.08	393
4	4	45	0.13	161
5	3	43	0.15	132
6	3	49	0.20	111
7	2	53	0.37	52
8	2	45	0.19	44
9	2	39	0.15	35
10	2	25	0.24	26
$nd\pi^1\Pi_g$ series				
4	6	45	0.17	246
5	5	49	0.17	162
6	4	45	0.12	99
7-	2	46	0.21	8
7+	2	59	0.13	102
8-	2	46	0.15	8
8+	2	49	0.18	83
9-	2	40	0.00	7
9+	2	47	0.28	85
10-	2	22	0.29	6
10+	2	35	0.34	55
11-	2	22	0.10	6
11+	2	31	0.18	51

accompaniment of correlations that adversely affect the rotational constants of the Π^- components. Therefore, the Π^- and Π^+ levels were analyzed separately. In two cases, ($10-11d\pi^1\Pi_g$) it was necessary to use an assumed value for the centrifugal distortion constant Y_{02} based on the relation

$$Y_{02} = -4 Y_{01}^3 / Y_{10}^2 \quad (2)$$

in order to circumvent the problem of limited Π^- data.

When comparing Dunham coefficients of electronic states within the same Rydberg series, it is desirable to use the same set of coefficients for fitting each state and to restrict the data bases to roughly the same range of ν and J since the Dunham coefficients are sensitive to these parameters. However, this procedure was used only sparingly in our analysis since only a few of the observed Rydberg states are useful for deriving the properties of the ground state of Li_2^+ . For the remaining Rydberg states, the advantage of having constants that fit all of the observed levels outweighs the desirability of using the same coefficients for all members of the series. The vibrational analyses of all $n > 7$ Rydberg states were restricted to two constants (Y_{10} and Y_{20}) and three vibrational levels ($\nu = 0-2$). The Π^- components of the $7-11d\pi^1\Pi_g$ states were additionally restricted to three rotational constants (Y_{01} , Y_{02} , and Y_{11}) but lambda-doubling interactions of the type $\Sigma^+ \leftrightarrow \Pi^+$ render restrictions in the rotational constants pointless for all other observed high-lying Rydberg states. The correlations between the rotational and vibrational constants in each Dunham fit are sufficiently small that restrictions did not have to be applied to the two subsets of constants simultaneously.

A summary of the most significant information contained in the above listings of Dunham coefficients is presented in Tables VI and VII. This listing includes several parameters that are not explicitly given in

TABLE VI. Selected molecular constants for the $nd\pi^1\Pi_g$ Rydberg states of $^7\text{Li}_2$. All of the constants listed for the $7-15d\pi^1\Pi_g$ states were derived exclusively from Π^- data except for the lambda-doubling constant q . All units are cm^{-1} except where indicated differently.

$nd\pi^1\Pi_g$ series								
n	T_0	T_e	ω_e	$\omega_e x_e$	B_e	α_e	r_e (\AA)	q
3	31 807.6	31 868.4	229.3	1.6	0.469	0.0055	3.20	0.001
4	35 299.7	35 360.8	229.0	2.1	0.474	0.0074	3.18	0.001
5	37 201.0	37 257.7	237.4	1.6	0.479	0.0060	3.17	0.002
6	38 410.1	38 460.9	249.3	1.6	0.486	0.0053	3.14	0.000
7	39 201.1	39 249.5	253.9	1.2	0.491	0.0053	3.13	-0.019
8	39 732.5	39 779.3	257.3	1.3	0.495	0.0047	3.12	-0.029
9	40 102.5	40 150.7	253.9	0.4	0.495	0.0040	3.12	-0.012
10	40 372.1	40 415.8	263.8	1.9	0.496	0.0071	3.11	-0.040
11	40 564.2	40 610.0	259.2	1.3	0.496	0.0039	3.11	-0.015
12	40 715.0	40 759.3	262.4	1.7				
13	40 832.4	40 876.7	262.2	1.3				
14	40 924.2	40 968.6	262.1	1.6				
15	40 998.6	41 042.3	263.8	2.2				

TABLE VII. Selected molecular constants for the $nd\sigma^1\Sigma_g^+$ and $ns\sigma^1\Sigma_g^+$ Rydberg states of ${}^7\text{Li}_2$. All units are cm^{-1} except where indicated differently.

$ns\sigma^1\Sigma_g^+$ series							
n	T_0	T_e	ω_e	$\omega_e x_e$	B_e	α_e	r_e (Å)
3	27 357.2	27 410.2	245.9	2.8	0.505	0.0096	3.09
4	34 253.2	34 293.6	270.7	2.9	0.480	0.0063	3.17
5	36 781.6	36 832.6	249.4	2.9	0.490	0.0100	3.13
6	38 079.0	38 129.1	251.8	4.1	0.486	0.0099	3.15
7	38 962.1	39 007.3	260.6	1.9	0.496	0.0044	a
8	39 580.2	39 624.4	262.5	1.6	0.492	0.0053	a
9	39 999.7	40 044.0	262.1	1.5	0.491	0.0044	a
10	40 295.4	40 339.5	262.7	1.6	0.481	0.0068	a
$nd\sigma^1\Sigma_g^+$ series							
3	33 268.9	33 321.1	246.8	2.1	0.465	0.0018	3.22
4	36 240.5	36 284.9	263.2	3.7	0.494	0.0054	3.12
5	37 793.4	37 890.1	145.7	-23.0	0.476	0.0104	3.18
6	38 520.3	38 571.8	247.6	1.1	0.497	0.0044	a
7	39 232.5	39 277.2	261.6	2.0	0.512	0.0044	a
8	39 753.8	39 798.7	261.0	1.6	0.529	0.0058	a
9	40 119.5	40 163.9	262.2	1.7	0.534	0.0062	a
10	40 382.5	40 426.9	261.9	1.4	0.546	0.0055	a

^a r_e is not given because B_e is substantially perturbed by lambda-doubling interactions.

Tables I–IV. The lambda-doubling constants that are presented in Tables VI and VII for the 7–11 $d\pi^1\Pi_g$ states have been computed from the relation

$$q = B_e(nd\pi^+) - B_e(nd\pi^-). \quad (3)$$

The constants listed for members $n=12$ –15 of the $nd\pi^1\Pi_g$ series had to be determined indirectly since the observations for each of these states consist of only one rotational level for each of the $v^*=0$ –2 vibrational

TABLE VIII. Comparison of corresponding atomic and molecular energy spacings in the Rydberg states of lithium. All values are in cm^{-1} units.

nd series			
n pair	$\Delta T_0(nd\sigma^1\Sigma_g^+)$	$\Delta T_0(nd\pi^1\Pi_g)$	ΔE (atomic)
3–4	2972	3492	5340
4–5	1553	1901	2472
5–6	727	1209	1342
6–7	712	791	809
7–8	521	531	525
8–9	366	370	360
9–10	263	270	258
10–11		192	189
11–12		151	147
12–13		117	113
13–14		92	89
14–15		74	72
ns series			
n pair	$\Delta T_0(ns\sigma^1\Sigma_g^+)$		ΔE (atomic)
3–4	6896		7806
4–5	2528		3287
5–6	1297		1688
6–7	883		980
7–8	618		619
8–9	419		416
9–10	296		295

levels. These values were calculated using the asymptotic values of the rotational constants obtained as described later.

Principal quantum numbers were assigned to each member of a particular Rydberg series by comparing the successive molecular potential well separations with energy differences between successive Li atomic levels.¹ This comparison is based on the assumption that the molecular dissociation energies of the high-lying Rydberg states are not significantly influenced by a distant Rydberg electron.¹⁵ It was found that corresponding atomic and molecular separations agree to within a few percent for $n > 6$ in all three observed Rydberg series. These separations are shown in Table VIII. The convention used for assigning n values to the molecular electronic states was the hydrogenic model.

For the $ns\sigma^1\Sigma_g^+$ Rydberg series, the procedure used for assigning n also fixes the azimuthal quantum number l since the energy spacings of the atomic s levels of Li are easily distinguishable from those of any other set of atomic Rydberg levels. However, this procedure cannot distinguish between different $l \neq 0$ series. Therefore, the remaining assignments could be made only by resorting to the argument that the strongest molecular transitions are expected to be those that correspond to allowed atomic transitions.¹⁵ Since the second step of all the OODR excitations originated at the $A^1\Sigma_u^+$ state, which dissociates to $\text{Li}(2s) + \text{Li}(2p)$, and since the $l=0$ series was separately identified, it was concluded that $l=2$ for both of the series that were not directly assignable.

All of the observed ${}^1\Sigma_g^+$ states were assigned to one of the two identified ${}^1\Sigma_g^+$ Rydberg series or to the doubly excited $\text{Li}(2p) + \text{Li}(2p)$ configuration. The identifications of the $E^1\Sigma_g^+$ and $F^1\Sigma_g^+$ state asymptotes have been confirmed by *ab initio* calculations.¹⁶ The ${}^1\Pi_g$ state cor-

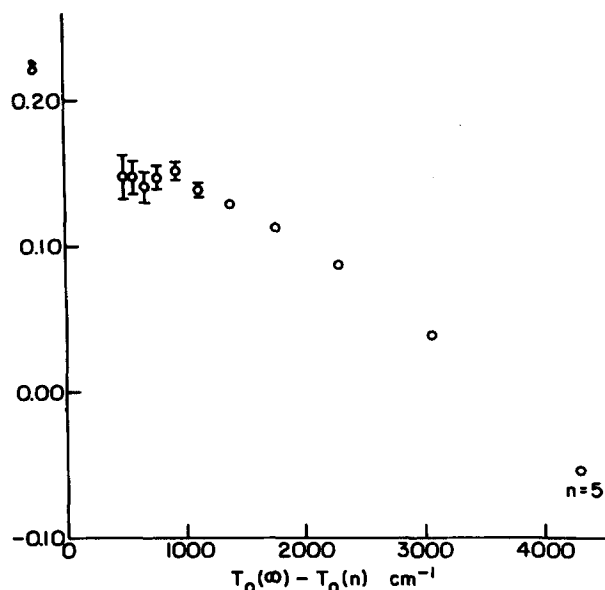


FIG. 2. The quantum defects δ of the Π^- components of the $nd\pi^1\Pi_g$ Rydberg states of ${}^7\text{Li}_2$. The δ values were calculated from the Rydberg equation for $T_0(\infty) = 41\,496\text{ cm}^{-1}$. The asymptotic behavior exhibited by δ in this plot indicates that the ionization potential is at its optimum value with respect to the observed spectral data.

relations are also straightforward except in two cases. First, none of the observed states can be identified with the doubly excited $\text{Li}(2p) + \text{Li}(2p)$ asymptote.¹⁷ Quantum mechanical calculations¹⁶ indicate that the molecular constants of this state differ markedly from those of any of the observed states. The second irregularity in the ${}^1\Pi_g$ state observations is the presence of a ${}^1\Pi_g$ state located about halfway between the $6d\pi^1\Pi_g$ and $7d\pi^1\Pi_g$ states. This state probably correlates with a doubly excited atomic configuration. It does not appear to be a member of a $\text{Li}(2s) + \text{Li}(nl)$ Rydberg series as no other series members were observed.¹⁸ Dunham coefficients for this state are included in Tables I–IV.

The electronic energies of several of the upper members of each Rydberg series were fitted with the molecular Rydberg equation:

$$T_0(n) = T_0(\infty) - R(n - \delta)^{-2}, \quad (4)$$

where n is the principal quantum number, δ is the quantum defect, and R is the Rydberg constant ($109\,733\text{ cm}^{-1}$ for ${}^7\text{Li}_2$). For a nonpenetrating orbital such as $nd\pi$, the quantum defect is expected to approach a constant as n increases.¹⁹ The optimum value for the ionization potential $T_0(\infty)$ is therefore determined by choosing trial values of this quantity until a plot of δ vs $T_0(\infty) - T_0(n)$ exhibits a plateau at large n .

The $nd\pi^1\Pi_g$ series provides the most reliable estimation of the ionization potential of Li_2 since the observations extend to a considerably higher n value in this series than in the two ${}^1\Sigma_g^+$ series. The extrapolation of the term energies of the $nd\pi^1\Pi_g$ components by the method described above yields $T_0(\infty) = 41\,496 \pm 4\text{ cm}^{-1}$. No rotational correction of this value is required since the

TABLE IX. Comparison of selected experimental and theoretical values for the ionization potential of Li_2 (cm^{-1} units).

Source	$T_0(\infty)$	Reference
OODR	$41\,496 \pm 4$	present work
<i>Ab initio</i>	$41\,630 \pm 200$	7
OODR ionization in a molecular beam	$41\,475 \pm 8$	21
OODR with two argon ion lasers	$41\,730 \pm 100$	23
Electron impact ionization	$39\,200 \pm 800$	25
	$39\,800 \pm 800$	24
Photoionization	$41\,500 \pm 800$	22
$B^1\Pi_u$, $C^1\Pi_u$, $D^1\Pi_u$ series extrapolation	40 250	26

virtual $v=0$, $J=0$ levels of the ${}^1\Pi_g^-$ components correlate with the $v=0$, $N=0$ level of the $X^2\Sigma_g^+$ state of Li_2^+ .²⁰ A plot of δ vs $T_0(\infty) - T_0(n)$ for $T_0(\infty) = 41\,496\text{ cm}^{-1}$ is shown in Fig. 2 for the $nd\pi^1\Pi_g$ series. A comparison of the above $T_0(\infty)$ value with corresponding values obtained from photoionization,^{21–23} electron impact ionization,^{24,25} *ab initio* calculations,⁷ and an earlier Rydberg extrapolation²⁶ is given in Table IX.

The values of $T_0(\infty)$ obtained from the $ns\sigma^1\Sigma_g^+$ and $nd\sigma^1\Sigma_g^+$ series data are consistent with the value stated above but are not as precise. Both series give a well-defined lower limit of $T_0(\infty) = 41\,490\text{ cm}^{-1}$. However, in both cases, the upper limit (approximately $41\,510\text{ cm}^{-1}$) can only be crudely estimated since it is impossible to determine whether or not δ reaches a plateau for $n < 11$ in these series. For $T_0(\infty) = 41\,496\text{ cm}^{-1}$, the limiting quantum defects for the $nd\pi^1\Pi_g$, $nd\sigma^1\Sigma_g^+$, and $ns\sigma^1\Sigma_g^+$ series are 0.15, 0.07, and 0.44 respectively. A summary of the quantum defects of the observed Rydberg states is given in Table X.

In addition to deriving values for $T_0(\infty)$ and δ , the Rydberg equation can be used to determine which of the observed states can be regarded as pure Rydberg states. If the Ritz relation $\delta = \alpha + \beta/n^2$ is assumed,²⁷ where α and β are adjustable constants, then the $T_0(n)$ values of members $n=7-9$ and $11-15$ of the $nd\pi^1\Pi_g$ series and members $n=7-10$ of the $ns\sigma^1\Sigma_g^+$ and $nd\sigma^1\Sigma_g^+$ series can be fitted with the Rydberg equation to within 1 cm^{-1} . The $T_0(n)$ value for the $10d\pi^1\Pi_g$ state cannot be fitted accurately because of a homogeneous perturbation.

TABLE X. Quantum defects for the observed Rydberg states of Li_2 .

n	$\delta (ns\sigma^1\Sigma_g^+)$	$\delta (nd\sigma^1\Sigma_g^+)$	$\delta (nd\pi^1\Pi_g)$
6	0.33	-0.07	0.04
7	0.42	0.04	0.09
8	0.43	0.06	0.11
9	0.44	0.07	0.13
10	0.44	0.07	0.14
11			0.15
12			0.15
13			0.14
14			0.15
15			0.15

TABLE XI. Deperturbed molecular constants for the Π^- components of the $9d\pi^1\Pi_g$ and $10\pi^1\Pi_g$ states.

n	T_0 (cm^{-1})	T_g (cm^{-1})	ω_g (cm^{-1})	$\omega_g x_g$ (cm^{-1})	B_g (cm^{-1})	α_g (cm^{-1})	r_g (\AA)	δ
10	40 367.7	40 412.2	261.9	1.7	0.497	0.0052	3.11	0.14
9	40 102.5	40 147.6	260.8	1.7	0.496	0.0052	3.12	0.13

Six of the states for which Dunham coefficients are listed in Tables I–IV contain a substantial number of energy levels that cannot be fitted satisfactorily with Eq. (1). These consist of members $n=9$ –11 of the $nd\pi^1\Pi_g$ series, $n=4$ –5 of the $nd\sigma^1\Sigma_g^+$ series, and $n=5$ of the $ns\sigma^1\Sigma_g^+$ series. Each of these states is discussed below.

The irregularities in the $9d\pi^1\Pi_g$ and $10d\pi^1\Pi_g$ data can be attributed to homogeneous perturbations of the $v+1$ vibrational levels of the $9d\pi^1\Pi_g$ state by the v levels of the $10d\pi^1\Pi_g$ state. These interactions can be described in terms of a model that was developed by Herzberg and Jungen to account for observed vibrational and rotational perturbations in Rydberg states of H_2 .²⁸ This model predicts strong homogeneous perturbations between closely lying pairs of $\Delta v=1$ vibrational levels belonging to a common Rydberg series. The $\Delta v=1$ perturbations have been formulated in terms of $d\delta/dr$, where r is the internuclear distance, and an explicit expression has been obtained which can be applied to $\Delta v=1$ interactions in any diatomic Rydberg series. The relative magnitudes of the observed $9d\pi^1\Pi_g(v+1) \leftrightarrow 10d\pi^1\Pi_g(v)$ perturbations in Li_2 were found to be in good agreement with the above model.

The homogeneous displacements of the $9d\pi^1\Pi_g$ vibrational levels were measured by fitting data from adjacent unperturbed Rydberg states with a Taylor-expanded form of the Rydberg–Ritz formula

$$T(n) = T(\infty) - Rn^{-2} + c_3n^{-3} + c_5n^{-5}, \quad (5)$$

where c_3 and c_5 are adjustable constants, and $T(n)$ is the sum of the electronic and vibrational energies of the n th Rydberg state. The downward displacements of the $9d\pi^1\Pi_g(v+1, J=0)$ levels [matched by the upward displacements of the $10d\pi^1\Pi_g(v, J=0)$ levels] are 4.4, 6.3, and 7.1 cm^{-1} , for $v=0, 1$, and 2, respectively. The interaction matrix element H can be determined for each of the interacting vibrational levels by means of the following relation, which is well known from perturbation theory²⁹:

$$H = \sqrt{\epsilon(\epsilon + \Delta E_0)}, \quad (6)$$

where ΔE_0 is the separation of the unperturbed pair of vibrational levels and ϵ is the magnitude of the displacement of either level from its unperturbed location. The H values corresponding to the above perturbations are 7.7, 10.8, and 13.3 cm^{-1} , respectively.

The rotational constants B_g and α_g of the $9d\pi^1\Pi_g$ component were deperturbed by applying two assumptions: (1) the $v=0$ level of the $9d\pi^1\Pi_g$ component is unperturbed since there is no $10d\pi^1\Pi_g$ vibrational level nearby; and (2) the α_g value for the $9d\pi^1\Pi_g$ component is approxi-

mately the same as the α_g values of nearby unperturbed Rydberg states. The B_g values for the $10d\pi^1\Pi_g$ component were deperturbed by assuming equal and opposite repulsions between the $9d\pi^1\Pi_g(v+1)$ and $10d\pi^1\Pi_g(v)$ levels. The results of the above procedures are presented in Table XI.

Additional homogeneous perturbations are likely to be present in most of the $n > 10$ states of the $nd\pi^1\Pi_g$ series but only those in the $11d\pi^1\Pi_g$ state were found to be significantly larger than the precision of measurement. An attempt to deperturb the $11d\pi^1\Pi_g$ state was abandoned when it became clear that a large number of possible perturbing states would have to be considered in the calculations.

The most unusual state that was observed was the $5d\sigma^1\Sigma_g^+$ state. The vibrational spacings in this state are expected to start at about 250 cm^{-1} and then slowly decrease. However, the first three observed vibrational spacings are 184, 208, and 219 cm^{-1} , respectively. This behavior suggests a repulsion of the lower vibrational levels of the $5d\sigma^1\Sigma_g^+$ state by an unidentified ${}^1\Sigma_g^+$ state lying at lower energy. Indeed, a fit of the neighboring $nd\sigma^1\Sigma_g^+$ states to a Rydberg formula indicates that the bottom of the potential well of the $5d\sigma^1\Sigma_g^+$ state is displaced upward by about 300 cm^{-1} . Despite the unusual vibrational structure presented by this state, there is good agreement between observed relative band intensities and calculated Franck–Condon factors.

Other unusual states include $4d\sigma^1\Sigma_g^+$ and $5s\sigma^1\Sigma_g^+$. The B_v values of each of these states decrease at a normal rate over the first few vibrational levels but then drop sharply at $v=3$ in the $5s\sigma^1\Sigma_g^+$ state and at $v=4$ in the $4d\sigma^1\Sigma_g^+$ state. Since such behavior cannot be represented accurately by a Dunham expansion, only the lowest few vibrational levels of the above two states were fitted with Eq. (1).

A noteworthy feature of the $nd\pi^1\Pi_g$ Rydberg series is the onset of large lambda doubling at $n=7$. This is consistent with the observation that the spacings between corresponding members of the $nd\pi^1\Pi_g$ and $nd\sigma^1\Sigma_g^+$ series are much larger for $n < 7$ than for $n \geq 7$. Furthermore, the observed behavior of the rotational constant B_v in each of these two series is consistent with the fact that the $nd\sigma^1\Sigma_g^+$ states lie higher in energy than the corresponding $nd\pi^1\Pi_g$ states. However, the B_v values for these states cannot be deperturbed simply by treating each nd complex as an isolated entity. The failure of conventional methods to handle similar perturbation problems in H_2 and He_2 has led to the development of multichannel quantum defect theory.²⁹ However, such a procedure is not essential in the present analysis since the rotational constants of the ground state of Li_2^+ can

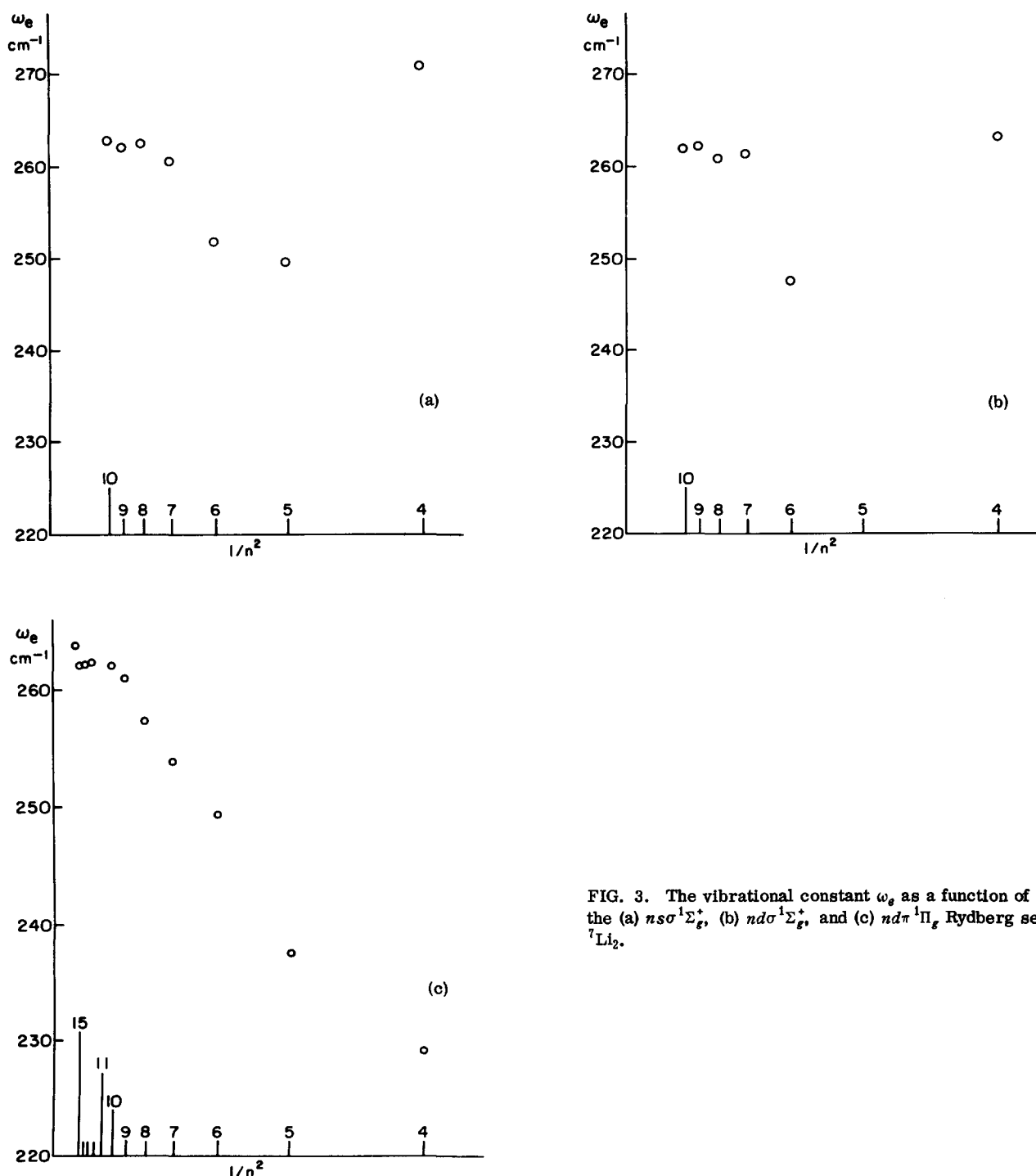


FIG. 3. The vibrational constant ω_e as a function of $1/n^2$ for the (a) $ns\sigma^1\Sigma_g^+$, (b) $nd\sigma^1\Sigma_g^+$, and (c) $nd\pi^1\Pi_g$ Rydberg series of ${}^7\text{Li}_2$.

be determined through examination of the Π^- components of the $nd\pi^1\Pi_g$ Rydberg states.

Accurate estimates of the vibrational constants of the ground state of Li_2^+ can be readily obtained from the observed molecular Rydberg states since these constants reach their asymptotic values within the range of experimentally observed states. This is illustrated in Fig. 3 by plots¹⁵ of ω_e vs $1/n^2$ for the three observed Rydberg series. (The quantity $1/n^2$ was chosen since the electronic energies of the Rydberg states are approximately functions of $1/n^2$.) The result of averaging the 11 ω_e values that lie near the asymptotes of these

plots is $\omega_e = 262.2 \pm 1.5 \text{ cm}^{-1}$. The average $\omega_e x_e$ value derived from these same states is $\omega_e x_e = 1.7 \pm 0.5 \text{ cm}^{-1}$. These values are in agreement with *ab initio* calculations.⁷ An alternative method of obtaining the foregoing results is to extrapolate the rotationless term energies of $v=0, 1$, and 2 of the $nd\pi^1\Pi_g$ states of Li_2 and use the three series limits to calculate ω_e and $\omega_e x_e$. The constants derived in this manner are in agreement with the values stated above but are less precise.

The extrapolations of the rotational constants are less reliable because of lambda-doubling perturbations. However, the Π^- components of the $nd\pi^1\Pi_g$ Rydberg

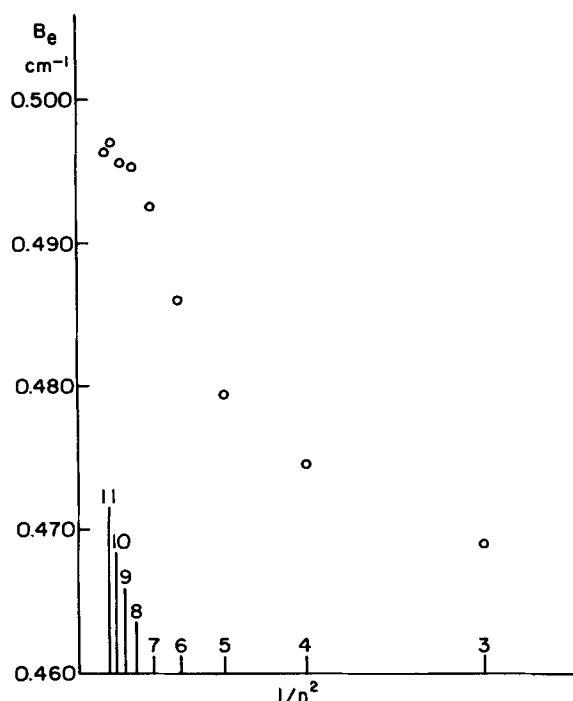


FIG. 4. The rotational constant B_e as a function of $1/n^2$ for the Π^- components of the $nd\pi^1\Pi_g$ Rydberg states of ${}^7\text{Li}_2$.

series are likely to be free of such interactions since the lowest lying ${}^1\Sigma_g^+$ state correlates with $\text{Li}(2p) + \text{Li}(3d)$, a configuration that lies more than 13 000 cm^{-1} above the highest vibrational level for which rotational constants have been obtained. Perturbations involving ${}^1\Delta_g^+$ states are also possible but are likely to be negligible since a plot of B_e vs $1/n^2$ for the $nd\pi^1\Pi_g$ series exhibits no significant irregularities. Additional evidence for the absence of large lambda-doubling perturbations in the $nd\pi^1\Pi_g^-$ components is that Eq. (2) is accurate to within 12% for all $nd\pi^1\Pi_g^-$ components for which data are available. On the other hand, this relation is inaccurate by as much as several hundred percent when applied to states for which substantial lambda-doubling interactions are known to be present.

The B_e values for the Π^- components of the $nd\pi^1\Pi_g$ states are summarized in Tables VI and VII, and plotted in Fig. 4. The asymptotic B_e value was obtained by adding one-half of the average α_e value to the average

TABLE XII. Comparison of experimental and theoretical spectroscopic constants of ${}^7\text{Li}_2^+ X^2\Sigma_g^+$ (cm^{-1} units).

Constant	OODR	<i>Ab initio</i> ^a
ω_e	262.2 ± 1.5	261.5
$\omega_e x_e$	1.7 ± 0.5	1.6
B_e	0.496 ± 0.002	0.491
α_e	$(5.2 \pm 1.7) \times 10^{-3}$	5.3×10^{-3}
D_e	$10\,469 \pm 6$	$10\,320 \pm 200$

^aReference 7.

TABLE XIII. Dissociation energies (cm^{-1}) for the observed Rydberg states of Li_2 .

n	$D_e (ns\sigma^1\Sigma_g^+)$	$D_e (nd\pi^1\Pi_g)$	$D_e (nd\sigma^1\Sigma_g^+)$
3	8 317	7 937	6 484
4	9 240	9 784	8 860
5	9 989	10 359	9 727
6	10 381	10 498	10 387
7	10 483	10 519	10 491
8	10 485	10 514	10 494
9	10 481	10 505	10 489
10	10 480	10 499	10 484
11		10 490	
12		10 488	
13		10 483	
14		10 480	
15		10 479	

B_0 value of members $n=8-11$ of the $nd\pi^1\Pi_g^-$ series. This procedure took advantage of the fact that the $v=0$ levels are the least perturbed levels in the $nd\pi^1\Pi_g$ states. The asymptotic value of α_e was obtained by averaging the values of all of the pure Rydberg states since this constant does not exhibit any discernable dependence on n , Λ , or on the amount of lambda doubling. The results obtained from the above procedures are: $B_e = 0.496 \pm 0.002 \text{ cm}^{-1}$ and $\alpha_e = (5.2 \pm 1.7) \times 10^{-3} \text{ cm}^{-1}$.

A summary of the estimated constants of the ground state of Li_2^+ is given in Table XII along with corresponding values obtained from *ab initio* calculations.⁷ Since past experience¹⁶ indicates that the theoretical constants are uncertain by several percent, the agreement between the two sets of constants can be regarded as very good. An interesting feature of these results is that Li_2^+ has a weaker force constant and longer bond length than Li_2 even though the molecular ion has a greater bond strength than the neutral molecule.

The dissociation energies of the Rydberg states of Li_2 can be readily determined by using the T_e values listed in Tables VI and VII along with the value³⁰ of $D_e = 8521.5 \pm 4 \text{ cm}^{-1}$ for the ground state of Li_2 . These D_e values are listed in Table XIII and plotted vs $1/n^3$ in Fig. 5 for each of the observed Rydberg series. The variation of D_e with $1/n^3$ becomes approximately linear at large n , as expected. The sign of the linear slope is given by the sign of the difference between the limiting molecular and atomic quantum defects. The sign of the slope at low n values is positive or negative depending on whether the Rydberg electron is bonding or antibonding, respectively. All of the plots in Fig. 5 correspond to the latter. Using the value $T_0(\infty) = 41\,496 \text{ cm}^{-1}$ and correcting for the difference in the zero point vibrational energies of the ground states of Li_2 and Li_2^+ , a value of $D_e = 10\,469 \pm 6 \text{ cm}^{-1}$ is obtained for the ground state of Li_2^+ . This is within the error limits of a recent value⁷ of $D_e = 10\,320 \pm 200 \text{ cm}^{-1}$ obtained from *ab initio* calculations.

Some of the bands in the upper ${}^1\Sigma_g^+$ states of Li_2 exhibit intensity anomalies similar to those reported in the Rydberg states of other diatomic molecules.³¹ The most conspicuous anomalies occur in the $n > 4 \text{ } ns\sigma^1\Sigma_g^+$

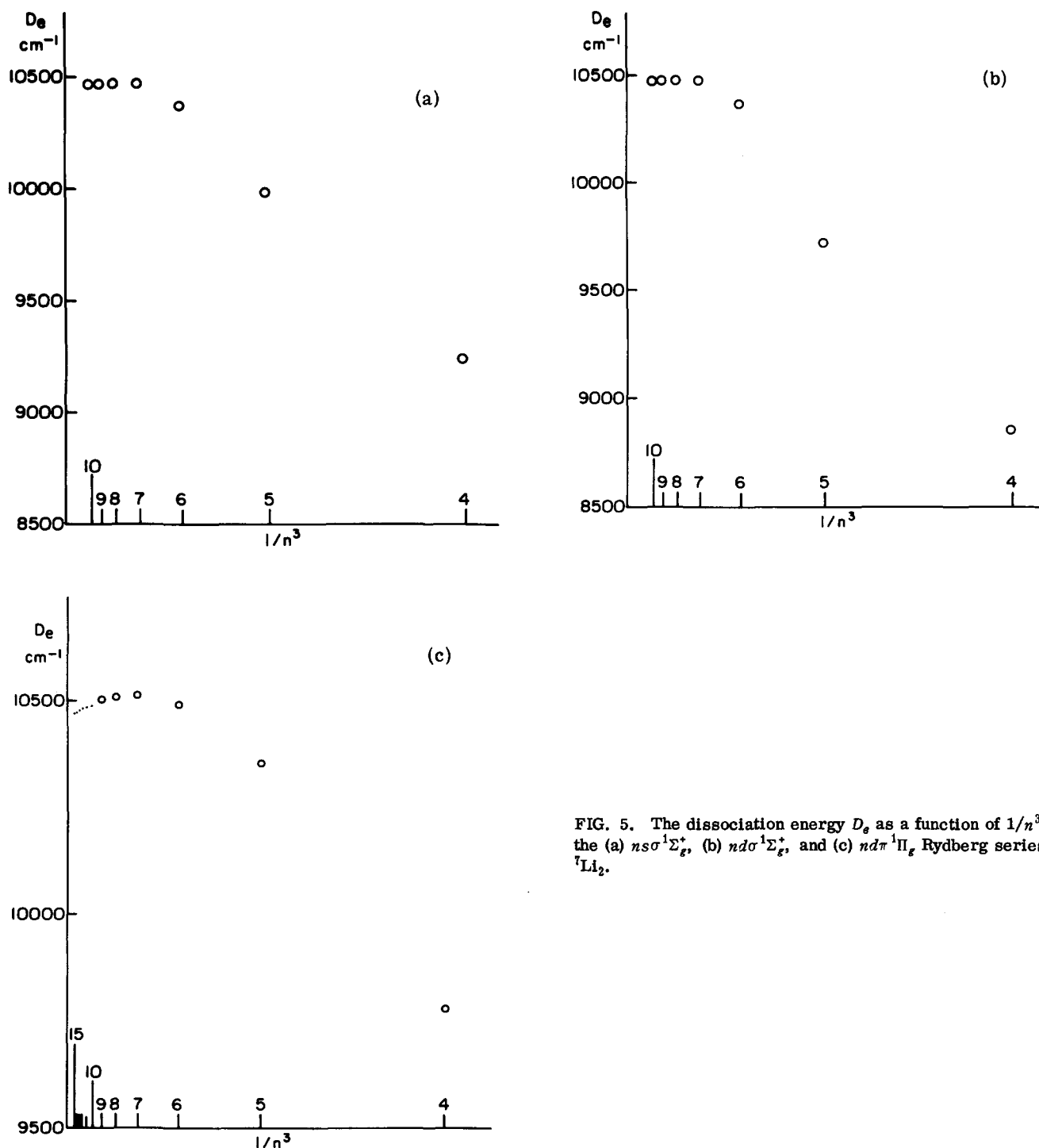


FIG. 5. The dissociation energy D_e as a function of $1/n^3$ for the (a) $ns\sigma^1\Sigma_g^+$, (b) $nd\sigma^1\Sigma_g^+$, and (c) $nd\pi^1\Pi_g$ Rydberg series of ${}^7\text{Li}_2$.

$-A^1\Sigma_u^+$ bands. Most of the P branches of these bands are much weaker than the corresponding R branches, especially at large J values. In some instances, the P branch is completely missing. The qualitative behavior of these perturbations is indicative of a mixing of ${}^1\Sigma_g^+$ and ${}^1\Pi_g$ states.³² For similar perturbations observed in other diatomic molecules, it is generally found that a weakening of the P branch usually occurs for the lower energy transition to one of two mutually perturbing $\Delta\Lambda = \pm 1$ states.³¹ This pattern suggests that the intensity anomalies found in the $ns\sigma^1\Sigma_g^+ - A^1\Sigma_u^+$ bands may be due to $ns\sigma^1\Sigma_g^+ \leftrightarrow nd\pi^1\Pi_g$ interactions. However, there

are no corresponding P/R intensity asymmetries in the $nd\pi^1\Pi_g - A^1\Sigma_u^+$ bands although both the P and the R branches are much less intense than the Q branch. In view of this complication, no further attempt was made to interpret the above anomalies.

IV. DISCUSSION

The present work exemplifies the usefulness of pulsed OODR since simplified spectra are essential for the efficient study of Rydberg states. Of the 36 electronic states of LiLi_2 that have now been characterized

experimentally, 31 are known as a result of OODR experiments. Previous work on Li_2 by single-photon excitation methods has failed to produce a reliable identification of any Rydberg series. Although it has been suggested²⁶ that the $B^1\Pi_u$, $C^1\Pi_u$, and $D^1\Pi_u$ states of Li_2 are members of the $n\pi^1\Pi_u$ series, it now appears likely³³ that the $C^1\Pi_u$ state correlates with $\text{Li}(2s) + \text{Li}(3d)$. In any event, the experimentally determined molecular constants for these states do not give accurate extrapolations to asymptotic values.

The lithium dimer is the second diatomic molecule for which a systematic study of Rydberg states has been performed by OODR. Results for the first such molecule Na_2 have been obtained by polarization-labeling spectroscopy,^{15,34} and by two-step autoionization in a supersonic molecular beam.^{35,36} The ${}^1\Sigma_g^+$ and ${}^1\Pi_g$ Rydberg series reported here correspond to those observed in Na_2 ^{15,34,35} but an attempt has not yet been made to locate the corresponding ${}^1\Delta_g$ series.^{15,34-36} It is interesting to note that, in analogy to our observations, the lowest doubly excited ${}^1\Pi_g$ state is reported to be missing from the polarization-labeled spectrum of Na_2 .¹⁵

ACKNOWLEDGMENTS

This work was supported by the National Science Foundation, the Donors of the Petroleum Research Fund, administered by the American Chemical Society, and the U.S. Naval Sea System Command under contract with The Pennsylvania State University Applied Research Laboratory.

¹R. A. Bernheim, L. P. Gold, P. B. Kelly, C. Kittrell, and D. K. Veirs, *Phys. Rev. Lett.* **43**, 123 (1979).

²R. A. Bernheim, L. P. Gold, P. B. Kelly, C. Kittrell, and D. K. Veirs, *Chem. Phys. Lett.* **70**, 104 (1980).

³R. A. Bernheim, L. P. Gold, P. B. Kelly, T. Tipton, and D. K. Veirs, *J. Chem. Phys.* **74**, 2749 (1981).

⁴R. A. Bernheim, L. P. Gold, P. B. Kelly, C. Tomczyk, and D. K. Veirs, *J. Chem. Phys.* **74**, 3249 (1981).

⁵R. A. Bernheim, L. P. Gold, P. B. Kelly, T. Tipton, and D. K. Veirs, *J. Chem. Phys.* **76**, 57 (1982).

⁶R. A. Bernheim, L. P. Gold, and T. Tipton, *Chem. Phys. Lett.* **92**, 13 (1982).

⁷D. D. Konowalow and M. E. Rosenkrantz, *Chem. Phys. Lett.* **61**, 489 (1979).

⁸L. Bellomonte, P. Cavaliere, and G. Ferrante, *J. Chem. Phys.* **61**, 3225 (1974).

⁹These results were obtained by pumping a Molelectron DL-300 dye laser with a 700 kW Molelectron UV-1000 N_2 laser.

¹⁰Exciton Laser Dyes, Exciton Chemical Company, Dayton, Ohio.

¹¹See AIP document No. PAPS JCPA-78-3635-47 for 47 pages containing observed spectral transitions, assignments, and differences between observed and calculated spectral energies. Order by PAPS number and journal reference from American

Institute of Physics, Physics Auxiliary Publication Service, 335 East 45th Street, New York, N.Y. 10017. The price is \$1.50 for microfiche or \$5 for photocopies. Airmail additional. Make check payable to the American Institute of Physics.

¹²P. Kusch and M. M. Hessel, *J. Chem. Phys.* **67**, 586 (1977).

¹³Observations of the $n=12-15$ states of the $nd\pi^1\Pi_g$ series were limited by low transition probabilities. For these states, only the strongest Q-branch line of each band was strong enough to be detected.

¹⁴C. E. Moore, *Atomic Energy Levels*, Natl. Bur. Stand. Circ. 467 (1949); N. Anderson, W. S. Bickel, G. W. Cariveau, K. Jensen, and E. Veje, *Phys. Scr.* **4**, 113 (1971).

¹⁵N. W. Carlson, A. J. Taylor, K. M. Jones, and A. L. Schawlow, *Phys. Rev. A* **24**, 822 (1981).

¹⁶D. D. Konowalow and J. L. Fish (private communication); D. D. Konowalow and J. L. Fish, *J. Chem. Phys.* **76**, 4571 (1982).

¹⁷The assignment of the $G^1\Pi_g$ state to the $\text{Li}(2s) + \text{Li}(3d)$ asymptote differs from the tentative $\text{Li}(2p) + \text{Li}(2p)$ assignment stated in an earlier paper (Ref. 3). It is interesting to note that the $G^1\Pi_g$ state may actually dissociate to the lower-lying $\text{Li}(2p) + \text{Li}(2p)$ configuration in accordance with the noncrossing rule.

¹⁸The lowest doubly excited configuration to which this state can dissociate is $\text{Li}(2p) + \text{Li}(3s)$, which would give $D_0 = 11\,646\text{ cm}^{-1}$. Franck-Condon factor calculations indicate that the preliminary vibrational assignments for this state are correct. There are so signs of any perturbations that might be causing this state to be observable solely on account of configuration mixing.

¹⁹M. L. Ginter and D. S. Ginter, *J. Chem. Phys.* **48**, 2284 (1968).

²⁰G. Herzberg, *Molecular Spectra and Molecular Structure*, 2nd ed. (Van Nostrand, Princeton, 1950), Vol. I.

²¹D. Eisel and W. Demtröder, *Chem. Phys. Lett.* **88**, 481 (1982).

²²P. J. Foster, R. E. Leckenby, and E. J. Robbins, *J. Phys.* **B 2**, 478 (1969).

²³B. P. Mathur, E. W. Rothe, G. P. Reck, and A. J. Lightman, *Chem. Phys. Lett.* **56**, 336 (1978).

²⁴A. M. Emel'yanov, V. A. Peredvina, and L. N. Gorokhov, *High Temp. (USSR)* **9**, 164 (1971).

²⁵C. H. Wu, *J. Chem. Phys.* **65**, 3181 (1976).

²⁶R. F. Barrow, N. Travis, and C. V. Wright, *Nature (London)* **187**, 141 (1960).

²⁷H. G. Kuhn, *Atomic Spectra* (Academic, New York, 1969).

²⁸G. Herzberg and Ch. Jungen, *J. Mol. Spectrosc.* **41**, 425 (1972).

²⁹U. Fano, *Phys. Rev. A* **2**, 353 (1970).

³⁰K. K. Verma, M. E. Koch, and W. C. Stwalley (to be published).

³¹Ch. Jungen, *J. Chem. Phys.* **53**, 4168 (1970).

³²R. A. Gottscho, J. B. Koffend, R. W. Field, and J. R. Lombardi, *J. Chem. Phys.* **68**, 4110 (1978).

³³M. Allegrini, A. Kopystynska, and L. Moi, *J. Chem. Phys.* **71**, 2324 (1979).

³⁴N. W. Carlson, A. J. Taylor, and A. L. Schawlow, *Phys. Rev. Lett.* **45**, 18 (1980).

³⁵S. Martin, J. Chevalere, S. Valignat, J. P. Perrot, M. Broyet, B. Cabaud, and A. Hoareau, *Chem. Phys. Lett.* **87**, 235 (1982).

³⁶S. Leutwyler, T. Heinis, M. Jungen, H. P. Harri, and E. Schumacher, *J. Chem. Phys.* **76**, 4290 (1982).